Interaction of Osteoblasts with Extracellular Matrix: Effect of Mast Cell Chymase (43595)

K. BANOVAC,*,[1] F. BANOVAC,[†] J. YANG,[‡] AND E. KOREN[§]

Departments of Orthopedics and Rehabilitation and Surgery,[‡] University of Miami School of Medicine, Miami, Florida 33101; Duke University, School of Engineering,[†] Durham, North Carolina 27706; and the Oklahoma Medical Research Foundation,[§] Oklahoma City, Oklahoma 73162*

Abstract. **We studied the effect of mast cell chymase on the interaction between osteoblasts and extracellular matrix. Chymase was purified from mast cell lysate by anion exchange chromatography. Osteoblasts were isolated from rat calvarias by collagenase digestion. Incubation of osteoblasts with mast cell lysate (40–170 μg/ml) or purified chymase (8–32 μg/ml) resulted in changes in cell-matrix interaction and cell morphology. Osteoblasts treated with chymase also showed a gradual detachment from the artificial substrata and from the biomatrix (collagen-digested rib fragment). A similar effect of mast cell chymase on the osteoblasts was found *in vitro* on endosteum of an intact parietal bone. Neutral protease inhibitors abolished the effect of both crude and purified enzyme preparations on the cell-matrix interaction. Mast cell chymase had no effect on osteoblast viability. The effect of enzyme on osteoblast proliferation was studied with lower concentrations of enzyme (0.2 μg/ml) in order to avoid cell detachment; there was no effect on either the metaphase index or on the number of cells after 5 days of incubation with chymase. Osteoblast attachment and cell spreading on different matrix proteins (fibronectin, vitronectin, extract of noncollagenous matrix proteins from rat bone) were significantly altered by their pretreatment with chymase. Matrix fibronectin of osteoblasts in culture as well as soluble vitronectin and fibronectin were digested by rat mast cell chymase.**

Our data suggest that mast cells through action of neutral protease chymase may alter molecules in extracellular matrix that are important in osteoblast adhesion, cell spreading, maintenance of cell morphology, and, most likely, cell function.

[P.S.E.B.M. 1993, Vol 203]

The mast cells are numerous in bone of patients with postmenopausal osteoporosis (1, 2) and in renal osteodystrophy (3, 4). These cells are also found in high numbers in bones of animals on a low calcium and low vitamin D diet (5) and in healing of fracture callus (6, 7). Nonetheless, the function of mast cells in bone remains unknown. Mast cells have an important role in allergic reactions; moreover, these cells also participate in a variety of other biological responses (8, 9). Activated mast cells release different secretory mediators; it is known that heparin, histamine, and neutral proteases are the most abundant substances released into the tissue upon activation of mast cells (8). Our previous study showed that a crude preparation of mast cell mediators had a significant effect on osteoblast morphology (10). These data indicated that mast cells might possess a substance(s) that was able to alter the adhesivity of extracellular matrix (ECM) and cell contact with ECM molecules. In the present study we evaluated the effect of mast cells on osteoblast interaction with ECM and found that the active component of the mast cell granules is a neutral protease able to modify the structural integrity of adhesive molecules important in maintaining osteoblast-matrix interaction.

Materials and Methods

Tissue culture flasks and flat bottom plastic plates were obtained from Linbro, Flow Laboratories (McLean, VA); the bottom surface area was 4 cm^2/well for 12-well plates, 2 cm^2/well for 24-well plates, and 0.32

[1] To whom requests for reprints should be addressed at Department of Orthopedics and Rehabilitation (D-27), University of Miami School of Medicine, P.O. Box 016960, Miami, FL 33101.

Received January 11, 1993. [P.S.E.B.M. 1993, Vol 203]
Accepted February 19, 1993.

0037-9727/93/2032-0221$3.00/0

cm^2/well for 96-well plates. Ficoll-Paque was obtained from Pharmacia Fine Chemicals (Piscataway, NJ); a Bio-Rad kit for protein determination and Dowex 1-2x anion exchange resin were obtained from Bio-Rad Laboratories (Richmond, CA). Glass coverslips were obtained from Corning Glass Works (Science Products Division, Corning, NY); 0.22-μm Millex GV filters were obtainedfrom Millipore Co. (Bedford, MA). BGJb medium (Fitton-Jackson modification), collagenase type II, rat parathyroid hormone (PTH) fragment 1-34, rat fibronectin, fetal bovine serum (FBS), antiactin antibodies, porcine trypsin, phenylmethylsulfonylfluoride (PMSF), demecolcine, and all standard chemicals were obtained from Sigma Chemical Co. (St. Louis, MO). Reagents for the immunofluorescence study of fibronectin, bovine chymotrypsin, and human antichymotrypsin were obtained from Calbiochem Corp. (La Jolla, CA). Histochemical analysis of alkaline phosphatase in osteoblasts was performed with the alkaline phosphatase leukocyte kit (Sigma Diagnostics, St. Louis, MO). Sprague-Dawley rats were purchased from Charles River Farms (Wilmington, MA).

Preparation of Mast Cell Lysate. Mast cells were obtained from rats (250–300 g) after lavage of peritoneal and pleural cavities (11). An enriched suspension of mast cells was prepared using Ficoll gradient separation. A cell suspension (25 ml) was centrifuged on 15 ml Ficoll at 450*g* for 6 min at room temperature. The pellet stained with toluidine blue (11) showed greater than 85% mast cells. The viability of the mast cells was more than 98%, as assessed be trypan blue exclusion. Cell lysate was obtained by freezing and thawing of mast cell suspension, as described by Young *et al.* (12). Supernatant was filtered through a 0.22-μm filter and used in the experiments as mast cell lysate.

Purification of Mast Cell Chymase. Enzyme was purified from an enriched suspension of mast cells (13, 14). Briefly, 25×10^6 mast cells in 0.01 *M* MES, at pH 6, containing 0.5 *M* NaCl were disrupted by freezing and thawing and applied to a 1.2 × 10-cm column containing Dowex 1-2x resin. The column was washed with 30 ml 0.01 *M* MES at pH 6 and 0.5 *M* NaCl; chymase was eluted with wash buffer containing 1 *M* NaCl. The pooled enzyme fractions ware concentrated by vacuum dialysis at 4°C, dialyzed against 0.001 *M* MES, pH 6, and stored at −40°C. The specific activity of the chymase, assayed by cleavage of benzoyl-L-tyrosine ethylester, was 30.5 ± 2 units/mg (mean ± SD; $n = 4$). Five micrograms of the purified chymase migrated as a single band at 28 kDa in sodium dodecyl sulfate-polyacrylamide gel electrophoresis (SDS-PAGE) under denaturing conditions (15).

Inhibition of the Enzyme. Inactivated enzyme was prepared by the addition PMSF to a final concentration of 5 m*M*. PMSF was dissolved in isopropyl alcohol and then mixed with serum-free BGJb medium (v/v). Mast cell lysate or purified chymase was preincubated with PMSF for 18 hr at 4°C. Free PMSF, after inhibition, was removed by extensive dialysis against phosphate-buffered saline (PBS) or BGJb medium. After dialysis, the enzyme preparations were incubated with osteoblasts. An identically treated aliquot of the enzyme preparation without enzyme inhibitor was used as a control. Inactivation of chymase with antichymotrypsin was performed in BGJb medium, pH 7.4, at room temperature for 20 min at a chymase/enzyme inhibitor molar ratio of 1:5 (16). The aliquots of the mixture were subsequently used in the studies of osteoblast attachment and spreading.

Purification of Vitronectin. Rat plasma (100 ml) was clotted by the addition of 2 ml of 1 *M* $CaCl_2$. After removal of the clot by centrifugation, 1 m*M* PMSF and 5 m*M* EDTA were added to the serum. This sample was applied to a Sepharose 4B column (2-ml bed volume; 2 ml/min) and then to a heparin-Sepharose column (5-ml bed volume; 2 ml/min). The eluate was added to 96 g of urea and adjusted to 200 ml with distilled water to obtain a final concentration of 8 *M* urea. After 2 hr at room temperature, the mixture was applied to the same heparin-Sepharose column. The final purification of vitronectin was performed as originally described by Yatogho *et al.* (17). The first three fractions eluted with 10 m*M* sodium phosphate buffer containing 0.5 *M* NaCl, 8 *M* urea, and 5 m*M* EDTA, pH 7.7, were combined and dialyzed overnight against PBS at 4°C. Purified vitronectin preparation migrated as 75 and 65 kDa in SDS-PAGE (15).

Extraction of Bone Matrix Proteins. Tissue extract was prepared as described by Termine *et al.* (18, 19). Femura and tibias were taken from male rats (250–350 g). Animals were sacrificed by exsanguination from the abdominal aorta under Nembutal anesthesia, and limbs were dissected immediately after death. Soft tissue and periosteum were removed mechanically, diaphyseal portions were dissected, and bone specimens were manually crushed and broken into small pieces. Bone fragments were washed with several changes of PBS containing 0.02 *M* PMSF; pieces of bone were then extracted with 4 *M* guanidium chloride containing 0.5 *M* EDTA and 50 m*M* Tris-HCl buffer (10 ml/g, wet weight), pH 7.4. Each extraction was performed at 4°C for 48 hr; after two extractions, the suspensions were pooled and centrifuged, and supernatant was dialyzed against 50 m*M* Tris-HCl at 4°C for 24 hr using a dialyzing bag with a 1000-Dalton molecular weight cut-off. All solutions used in the extraction contained the following enzyme inhibitors: 0.1 *M* 6-aminohexanoic acid, 5 m*M* benzamidine hydrochloride, and 20 m*M* PMSF. The dialysis samples were then aliquoted and stored at −40°C. Consistent with the previous report by Termine *et al.* (20), SDS-PAGE analysis of the extract

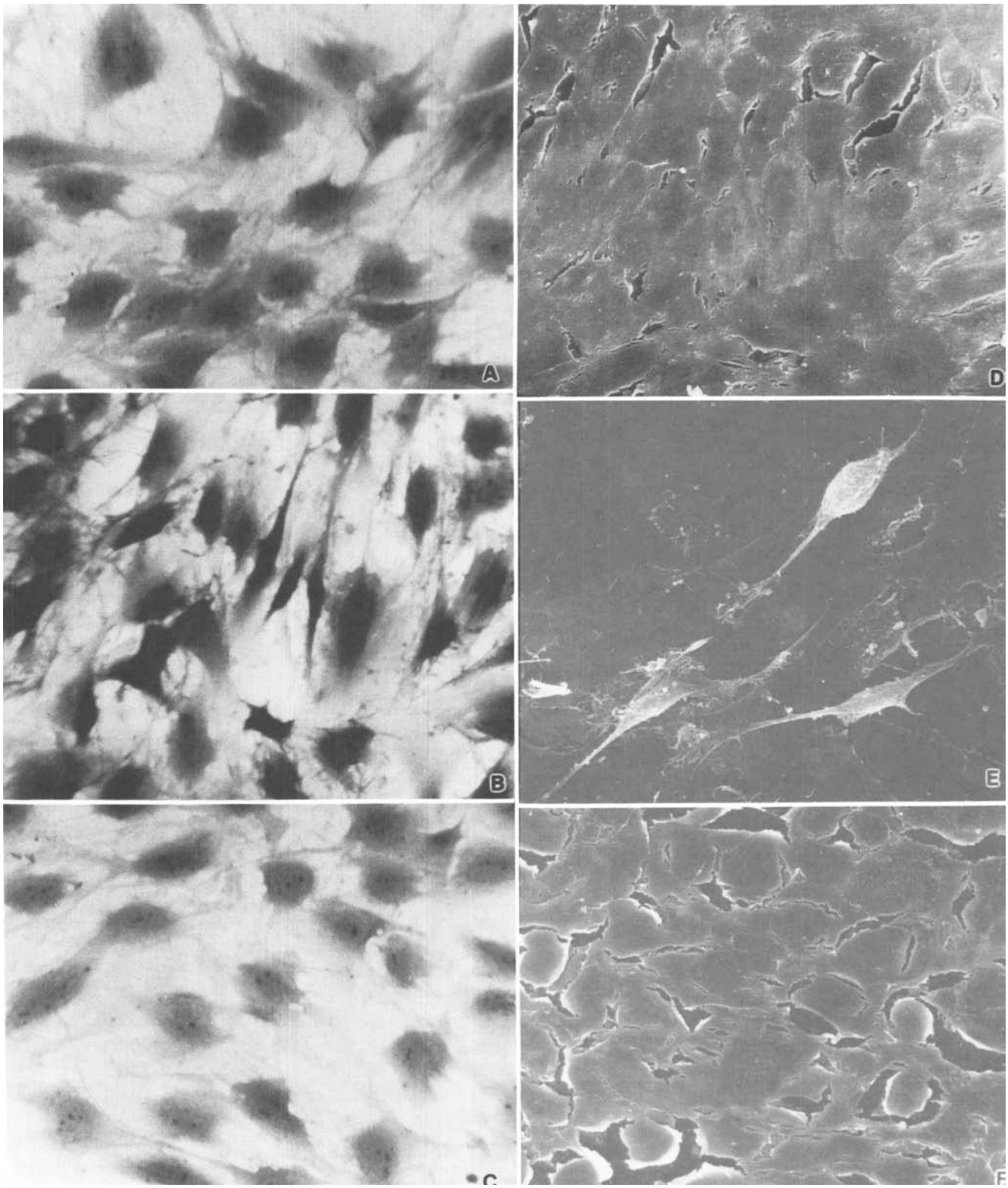

Figure 1. Effect of mast cell chymase on osteoblast-matrix interaction. Cells (2×10^4/well) in BGJb medium with 10% FCS were seeded to 24-well plates containing glass coverslips and incubated for 48 hr at 37°C in a 5% CO_2 atmosphere. Before the addition of 0.2 ml of chymase preparation (8 μg/ml; 15 min at 37°C), wells were rinsed with serum-free medium. Samples were prepared for analysis as described in Materials and Methods. The light micrographs are on the left; scanning electron micrographs are on the right. (A) and (D) Control; (B) and (E) chymase; (C) and (F) chymase pretreated with neutral protease inhibitor PMSF (5 m*M*). Note the similar morphology of osteoblasts in control samples and those exposed to chymase pretreated with PMSF. Intact chymase induced a fusiform appearance and cell retraction in some cells.

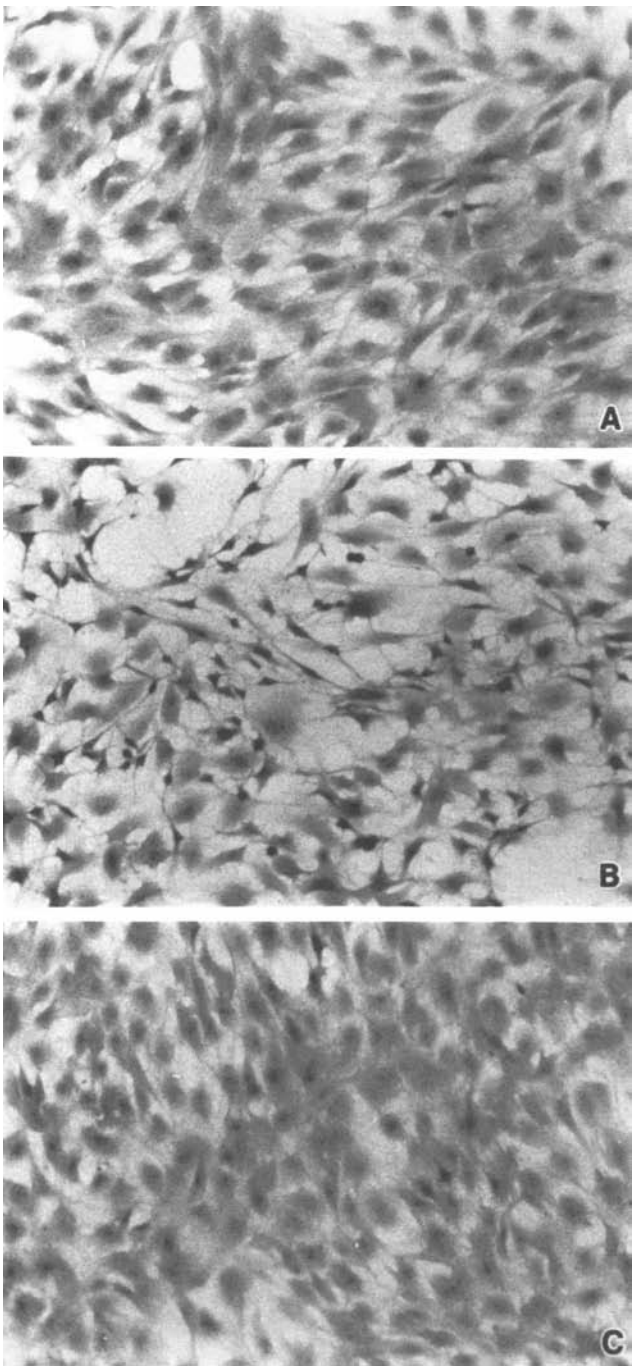

Figure 2. Effect of mast cell lysate on osteoblast-matrix interaction. Rat osteoblasts (2×10^4/well) in BGJb medium with 10% FCS were seeded to 24-well plates containing glass coverslips and incubated at 37°C in a 5% CO_2 atmosphere. At the subconfluent stage, 0.4 ml of mast cell lysate (170 μg protein/ml) was added to cells for 30 min. Samples were prepared for analysis as described in Materials and Methods. (A) Control; (B) mast cell lysate; (C) mast cell lysate pretreated with neutral protease inhibitor PMSF (5 m*M*). Magnification ×160; toluidine blue staining. Note the spindle-shaped appearance and cell retraction in some cells exposed to mast cell lysate.

revealed five dominant bands at approximate molecular weights of 65, 60, 42, 38, and 8 kDa.

Studies of Osteoblast-Matrix Interaction. Enriched suspension of osteoblasts was obtained from rat calvaria by digestion with collagenase using a minor modification of the method of Wong and Cohn (21). Calvarias were dissected from 1-day-old rats and digested in a solution containing 2000 units of collagenase II, 0.35 mg of trypsin, and 4 m*M* EDTA. The viability of isolated cells was greater than 98%, as determined by trypan blue exclusion. The phenotype of osteoblasts was evaluated by staining for alkaline phosphatase using naphthol-AS-BI phosphate as substrate (72 ± 5% of cells were positive) and by response to PTH (22). PTH (10^{-7} *M*) increased the cAMP production of osteoblasts to 1300% of the baseline value. The first four passages of osteoblasts, fractions 3 and 4 (21), were used for experiments. Cells were incubated in BGJb medium with 10% FBS in tissue culture 24- or 96-well plates at 37°C in humidified 5% CO_2 atmosphere.

The effects of mast cell chymase on ECM and on matrix interaction with osteoblasts were studied in three different systems: (i) planar substrate; (ii) bone matrix; and (iii) intact bone.

Cell culture on a planar substrate. Cell suspension in BGJb medium with 10% FBS was seeded to 24-well plastic culture dish or wells containing glass coverslips at 37°C in humidified 5% CO_2 atmosphere. Different matrix proteins were used to coat a planar surface, as indicated below. Before the addition of the enzyme or mast cell lysate, the serum-supplemented medium was removed, and the wells were washed with serum-free medium; the cell culture was then exposed to enzyme preparation. After exposure to the enzyme, cells were fixed with 3% formaldehyde and stained with toluidine blue (10).

Cell culture on bone matrix. Osteoblast suspension (2×10^4) in BGJb medium with 10% FCS was added to a well containing a collagenase-digested bone fragment and incubated for 5 days at 37°C in a CO_2 incubator. A rat rib fragment was digested with collagenase over a period of 24 hr; residual bone matrix containing no cells detectable by scanning electron microscopy (SEM) was used for experiments. After incubation, the medium was removed, and the wells were washed with a serum-free medium. Then, 0.4 ml of mast cell lysate (170 μg protein/ml) was added for 6 hr. The control samples were incubated in BGJb medium alone and treated in the same way as the samples treated with lysate. Incubation was terminated by fixation in 3% glutaraldehyde for SEM analysis (10).

Culture of intact bone. To study the effect of mast cell lysate on endosteal lining cells, the intact bone was incubated with an enzyme preparation. Bone specimens were obtained from rat calvaria of 4-week-old rats, as described above. The adherent tissue and periosteum

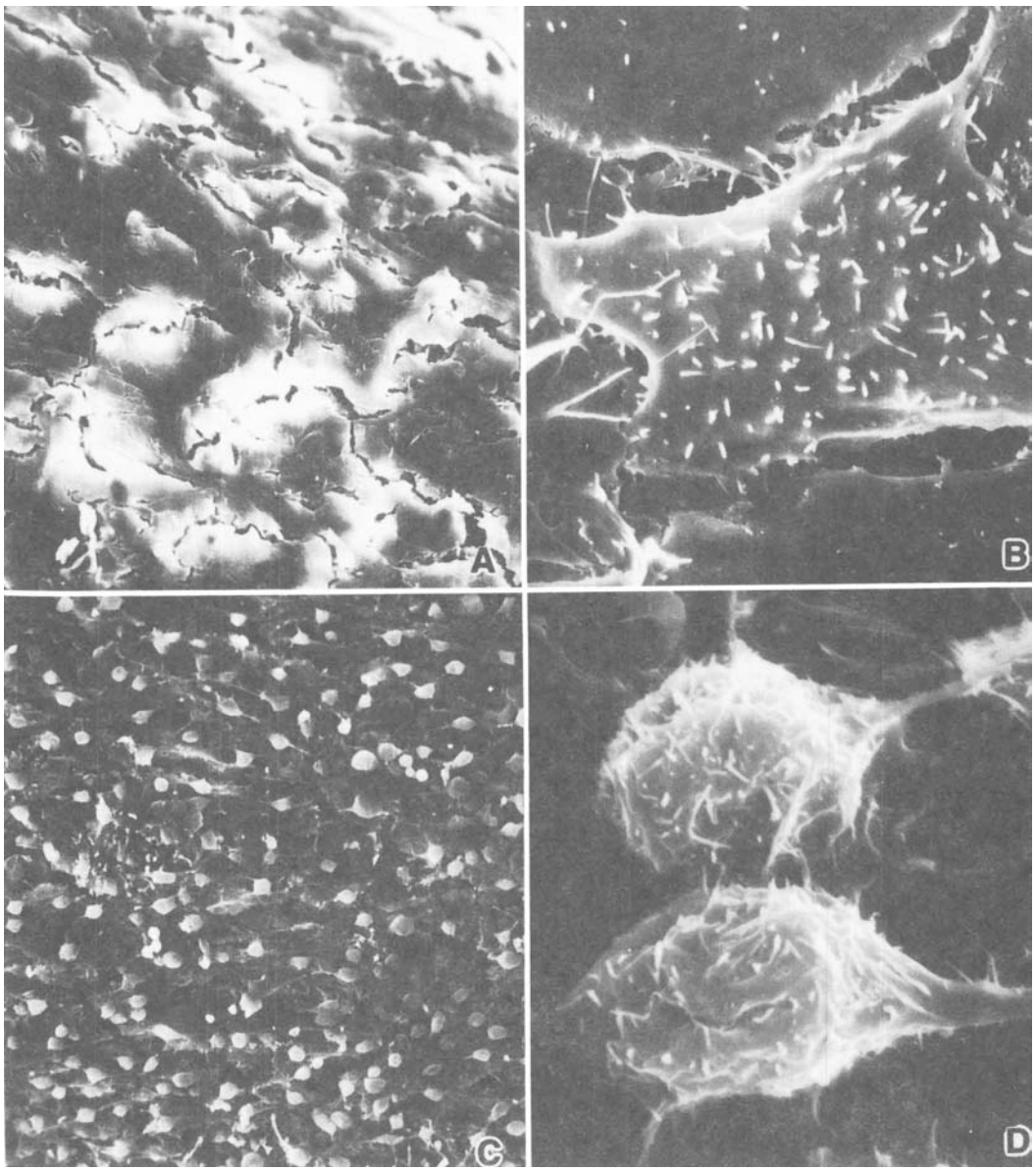

Figure 3. Scanning electron micrograph of isolated osteoblasts cultured on collagenase-digested bone fragment. Osteoblasts (2×10^4 cells) in BGJb medium with 10% FCS were added to 24-well plates containing enzyme-digested rib fragment for 5 days at 37°C in a CO_2 atmosphere; after incubation, wells were rinsed with serum free-medium, and 0.4 ml of mast cell lysate (170 μg protein/ml) was added for 6 hr; samples were prepared for SEM as described in Materials and Methods. (A) Control (×200 magnification); (B) control (×4000); (C) MCL (×200); (D) MCL (×4000). Note the changes in cell morphology after exposure to MCL; flat and well-spread cells on the substrate show different stages of cell detachment after exposure to MCL.

were removed with forceps under a dissecting microscope. Individual bones were preincubated in 24-well plates with 2 ml of BGJb medium supplemented with 10% FBS for 1 hr at 37°C. After removal of the medium, wells were rinsed with a serum-free medium, and 0.5 ml of mast cell lysate (170 μg protein/ml) was added in triplicate wells. Using scissors, a portion of the bone was removed from each bone fragment after 1, 6, and 24 hr of incubation; the endocranial aspect of the bone was prepared for SEM.

Cell Attachment Assay. The attachment of osteoblasts on matrix protein-coated plastic was studied by the method of Bourdin and Ruoslahti (23). Tests were carried out in 96-well flat bottom plates. The wells were coated with varying concentrations of fibronectin or vitronectin in PBS for 1 hr at 37°C. Both the chymase (16 μg/ml) and the medium (control) were added in triplicate wells and removed after 30 min. To study the effect of enzyme inhibition, the same amount of chymase pretreated with antichymotrypsin was added to the wells for 30 min. After rinsing with PBS, the wells were treated with 0.1 ml of 2% BSA for 30 min in order to block the nonspecific binding sites on the plastic surface. The plates were washed with PBS, and then 5

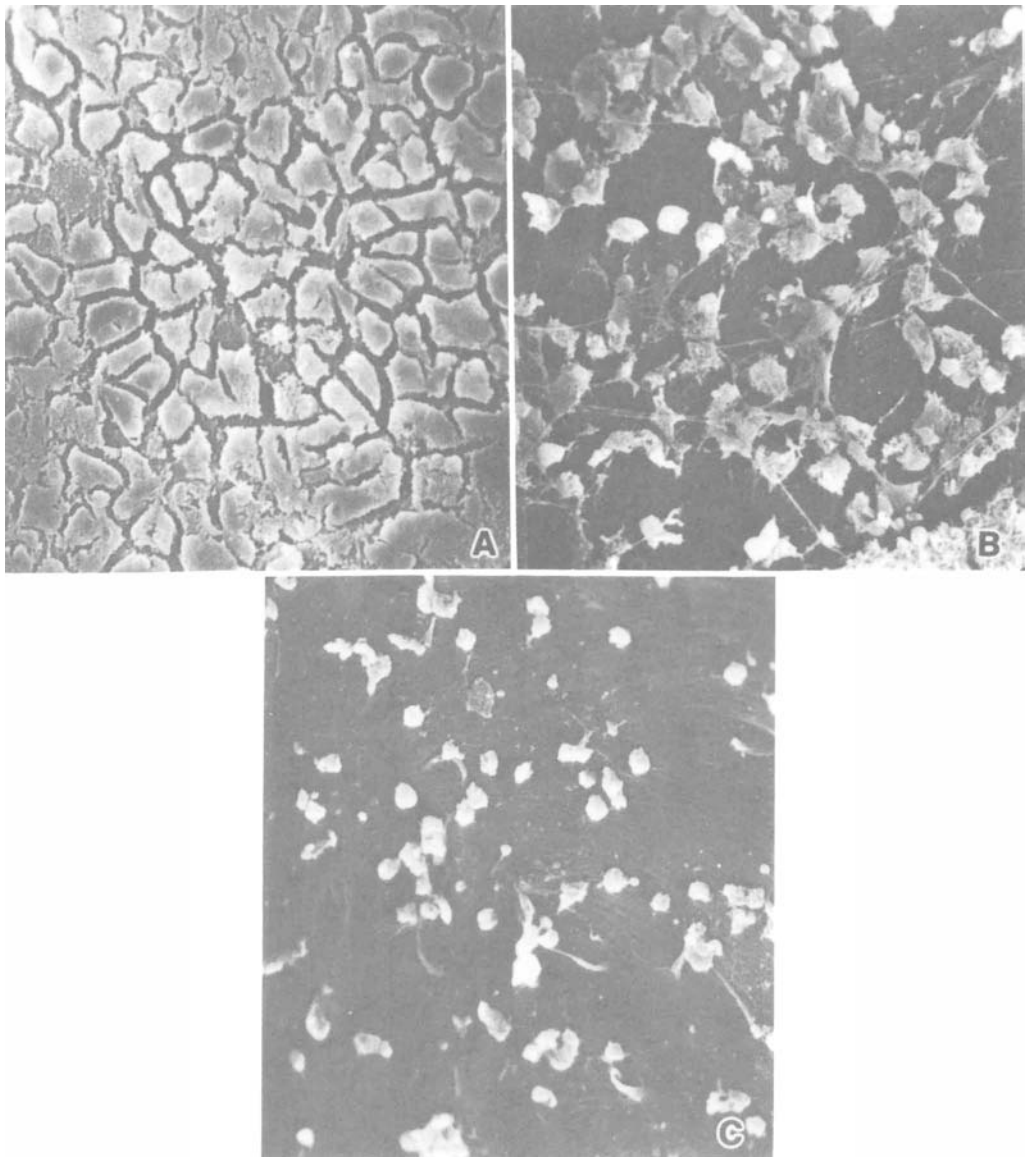

Figure 4. Scanning electron micrographs of intact parietal bone treated with MCL (×500 magnification). Bone was obtained from 4-week-old rats and incubated in 2 ml BGJb medium with 10% FCS for 1 hr at 37°C. After removal of medium, 0.5 ml of mast cell lysate (170 μg of protein/ml) was added; bone specimens were removed at different time intervals as described in Materials and Methods. (A) MCL (zero time); (B) MCL (1-hr incubation); (C) MCL (6-hr incubation). Control flat cells on matrix (A) after exposure to MCL show a reduction in size, larger areas of matrix between the cells, and spherical appearance of cells (B and C).

Table I. Effect of Chymase on Mitosis of Osteoblasts

	Metaphase index (%)
Control (n = 4)	0.3 ± 0.14
Chymase (n = 4)	0.5 ± 0.14
5% FCS (n = 4)	3.5 ± 0.28[a]

Quiescent cells were incubated in 1 ml of BGJb medium alone (control) or with chymase (0.2 μg/ml) or 5% FCS for 4 days at 37°C in a CO_2 atmosphere; osteoblasts were prepared for analysis as described by Malinin (28); results are presented as the mean ± standard deviation, expressed per 1000 cells. n = Number of experiments.
[a] $P < 0.001$ *vs.* control and chymase (analysis of variance).

× 10^4 cells in the BGJb medium containing 0.5% BSA were plated/well. The assays were carried out at 37°C in a CO_2 incubator for 90 min. Nonadherent cells were removed by washing with PBS, and adherent cells were fixed with 3% formaldehyde and stained with 0.5% toluidine blue. The relative number of adherent cells was determined after cell lysis with 1% SDS and expressed as the optical density of dye absorbance at 620 nm measured in an automatic spectrophotometer (23, 24).

Cell Spreading. The morphologic characteristics of cell spreading were studied by SEM on vitronectin, fibronectin, and bone matrix proteins. Cells were seeded to 12- or 24-well plates containing glass cover-

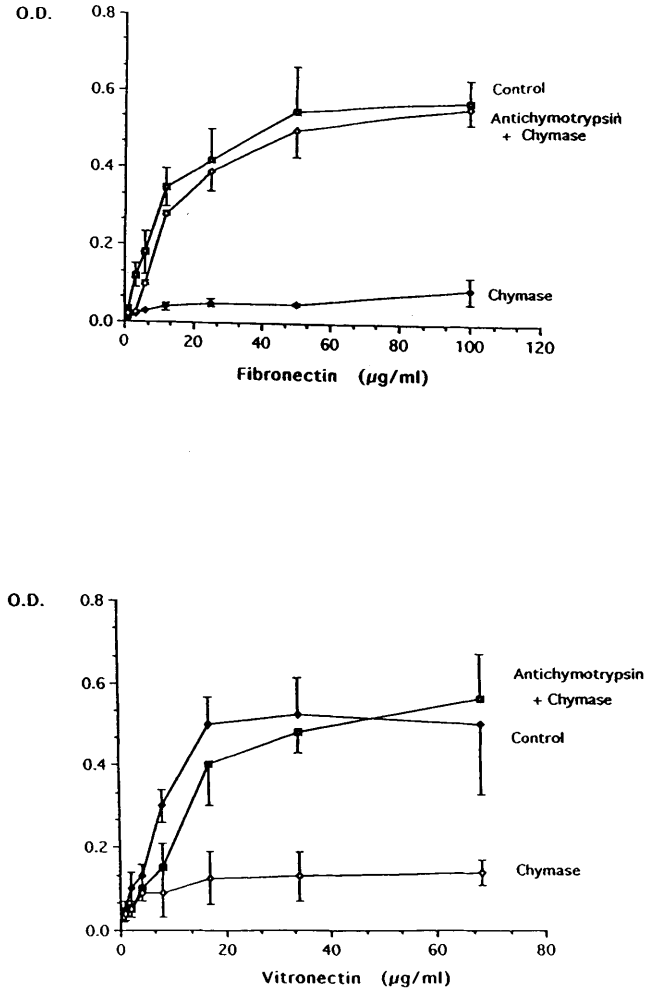

Figure 5. The effect of chymase on cell attachment. Plastic 96-well plates were coated with 50 μl of varying concentrations of fibronectin (0–16 μg/cm^2; 0–100 μg/ml) or vitronectin (0–11 μg/cm^2; 0–70 μg/ml) for 1 hr at 37°C. Coated wells were treated with 50 μl of chymase (16 μg/ml), a mixture of chymase and antichymotrypsin (1:5 molar ratio), or the medium (control) for 30 min before the addition of cells (1.5×10^4/well). Cells were allowed to attach for 90 min, the unbound cells were removed, and the number of attached cells was determined as described in Materials and Methods. Bars indicate the mean ± standard deviation of one representative experiment (n = 5). O.D., Optical density.

slips. Then, 0.2 ml of vitronectin or fibronectin dissolved in PBS was used for coating (0.5 μg/cm^2) at 37°C for 60 min. Upon washing with the serum-free medium, 0.2 ml of mast cell chymase (8 μg/ml) or medium (control) was added in parallel for 30 min. The wells were rinsed with PBS, and osteoblasts resuspended in BGJb medium containing 0.4% BSA were pipetted into the wells. In the experiments in which bone matrix proteins were used as a coating substrate, the cells were first allowed to attach to the surface for 24 hr, the enzyme preparation was then added, and incubation was extended for 48 hr. At the end of incubation, cells were fixed with 3% glutaraldehyde for SEM (10).

The quantitative analysis of cell spreading included: (i) determination of the percentage of spread osteoblasts; and (ii) measurement of cell surface area. For determination of cell spreading, osteoblast culture was prepared as described above. Cells were fixed with 3% formaldehyde, and cell spreading was determined using the method of Grinnell *et al.* (25); the data are expressed as the mean ± standard deviation of triplicate samples. To evaluate the effect of chymase on cell surface area, osteoblasts were seeded on glass coverslips. At the subconfluent stage, the cells were rinsed and exposed to 0.2 ml of chymase preparation (16 μg/ml) for 15 min at 37°C. After incubation, the cells were washed with PBS, fixed, and prepared for analysis of intracellular actin distribution using a modification of a previously reported method (26). The cells were first fixed with 3% paraformaldehyde for 30 min and then made permeable with 0.5% Triton X-100 in PBS for 15 sec. Before the addition of actin antibodies, nonspecific binding sites were blocked with 2% normal rabbit serum for 20 min. Rabbit antiactin (1:40) in PBS was added for 60 min. After incubation, the cells were washed, and goat antirabbit immunoglobulin G-fluorescein isothiocyanate (FITC) conjugate (1:100) was added for 45 min. The coverslips were washed with PBS after the final incubation, then mounted using glycerol. The quantitative analysis of the surface area of cells was determined by digital imaging fluorescence microscopy using an interactive laser cytometer ACAS-570 (Meridian Instruments, Okemos, MI) (27). The FITC-stained cells were scanned using the excitation laser light of 488 nm. The emitted fluorescence was measured after a passage through a 540 FWHM 10-nm filter (Melles Griot, Irvine, CA). On the basis of the fluorescence intensity measured in individual cells, an ACAS 570 computer provided cell scans as well as average fluorescence values, expressed in fluorescence units/μm^2 and average cell surface area in μm^2.

Digestion of Fibronectin and Vitronectin. Digestion of fibronectin or vitronectin in PBS buffer at pH 7.4 with rat mast cell chymase was performed at enzyme/substrate ratios of 1:70 and 1:50 (w/w), respectively. Samples of 1 ml were incubated at 37°C, and aliquots were withdrawn at given time intervals. The digestion was terminated by the addition of Laemmli's buffer and immediate freezing. The digestion products were analyzed by SDS-PAGE (15). After electrophoresis, the gels were stained with Coomassie brilliant blue.

Immunofluorescence Studies of ECM. Rat osteoblasts (4×10^4 cells/well) were grown in 24-well plates with coverslips in BGJb medium supplemented with 10% FBS. At the subconfluent stage, cells were washed with serum-free medium and then incubated with 0.2 ml of mast cell lysate (MCL; 150 μg/ml) or chymase preparation (33 μg/ml). After 2 hr of incubation with MCL and 20 min with chymase, cells were fixed with 3% paraformaldehyde and then an indirect immunofluorescence technique was used (28). To reduce nonspe-

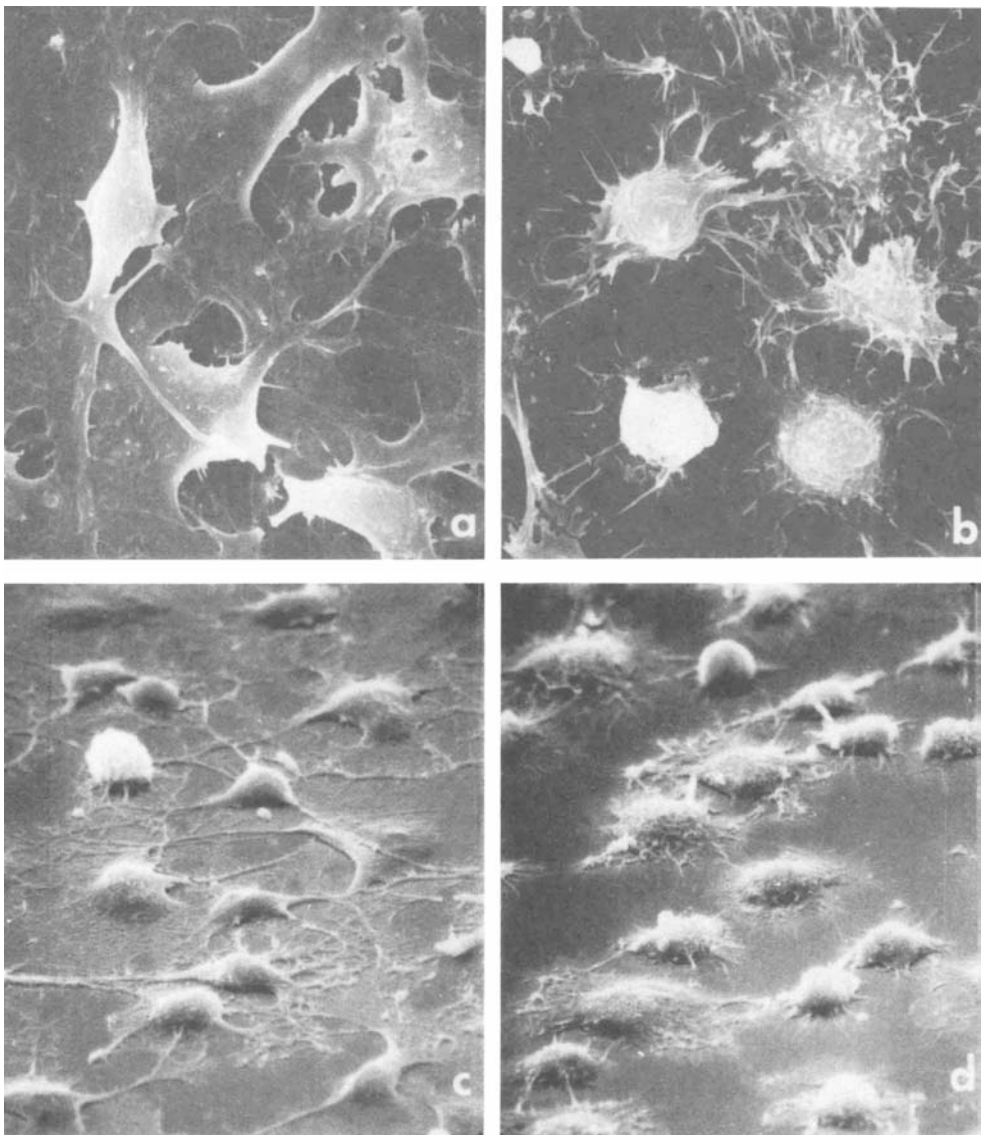

Figure 6. Scanning electron micrographs of osteoblast spreading on vitronectin. Glass coverslips were coated in 24-well plates with 0.2 ml of vitronectin (5 μg/ml; 0.5 $\mu g/cm^2$) for 1 hr at 37°C. After washing with serum free-medium (0.2 ml), either chymase (16 μg/ml) or the medium (control) was added for 30 min, followed by osteoblasts (4×10^4 cells/well) in BJGb medium with 0.4% BSA for 24 h as described in Materials and Methods. (A) and (C) Intact vitronectin; (B) and (D) chymase-treated vitronectin (magnification ×560). (A) and (B) represent micrographs taken at a 0° angle; (C) and (D) show a 60° angle. Note more rounded cells with limited spreading and a reduction of intercellular connections in cells seeded on enzyme-treated vitronectin (B and D).

cific antibody binding, avidin (1:100) was added for 30 min, and then coverslips with cells were incubated with goat antirat fibronectin serum (1:40) for 2 hr. Biotinylated rabbit antigoat immunoglobulin G (1:80) was added for 45 min, and final incubation with FITC-avidin (1:100) was carried out for 30 min. A Zeiss Universal microscope (Zeiss, New York, NY) with filters for FITC was used; fluorescence micrographs were made on Kodak film (Eastman Kodak, Rochester, NY).

Other Studies. The relative number of cells was determined in duplicate or triplicate wells after staining with toluidine blue and cell lysis with 1% SDS (23, 24). The dye absorbance was measured at 620 nm in an automatic spectrophotometer. The metaphase index of osteoblasts on coverslips after exposure to chymase was determined as described by Malinin (29). The viability of cells, detached from the substrate into the medium upon treatment with mast cell enzyme, was studied by: (i) trypan blue exclusion; (ii) reculturing of the cells in BGJb medium with 10% FBS; and (iii) SEM. The protein concentration was determined by the method of Bradford using a commercial kit.

Results

Effect on Osteoblast-Matrix Interaction. The effect of purified chymase on the osteoblast-matrix interaction and the effect of enzyme inhibition were studied on glass substrate. The morphologic changes were ana-

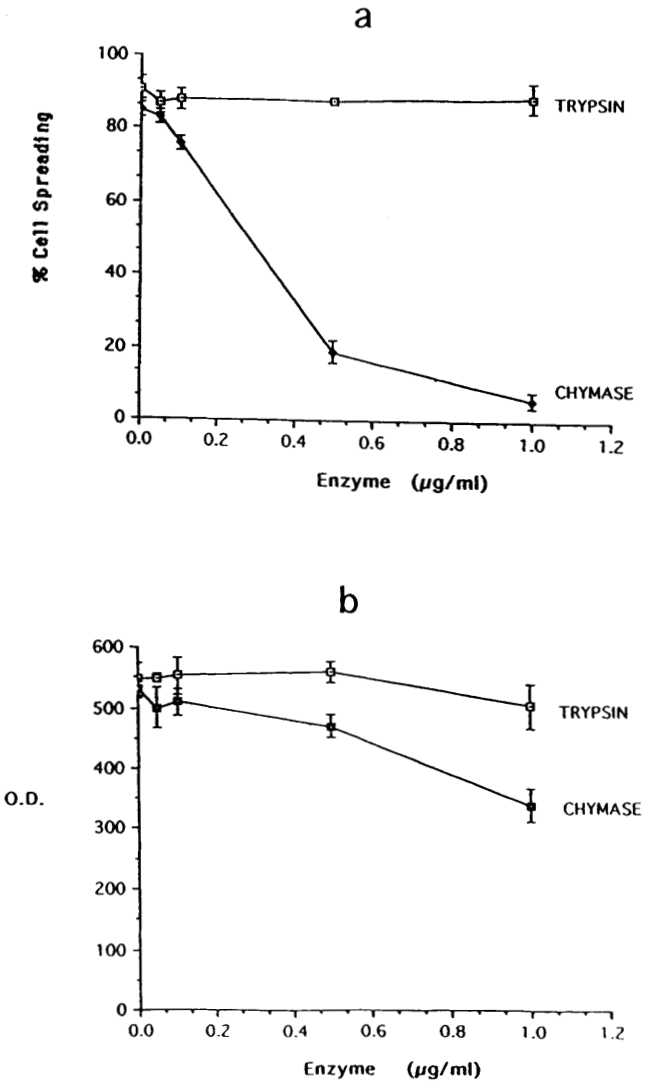

Figure 7. Dose-dependent effect of chymase on osteoblast spreading. Plastic 24-well plates were coated with 0.5 ml bone extract (10 μg/ml; 2.5 μg/cm^2) for 60 min at 37°C, and osteoblasts (2×10^4 cells/well) in BGJb medium with 0.4% BSA were added for 24 hr. After incubation, wells were washed with medium and treated with 1 ml of varying concentrations of enzyme (0–1 μg/ml). Cell spreading and number were determined as described in Materials and Methods. Bars indicate the mean ± standard deviation of one representative experiment ($n = 3$). Panel a presents the percentage of spread cells; panel b shows the effect on cell number (determined as optical density [O.D.] at 620 nm; see Materials and Methods).

lyzed by light and scanning electron microscopy. In these experiments, FBS was used to coat the glass surface. After 2 days, the cells covered the surface in a monolayer and displayed a flat polygonal shape (Fig. 1, A and C). The addition of purified enzyme for 15 min (Fig. 1, B and E) induced cellular and nuclear retraction and an appearance of spindle-shaped osteoblasts. Prolonged incubation with enzyme (1–2 hr) resulted in the detachment of cells from the substrate. After enzyme inhibition with the protease inhibitor PMSF (Fig. 1, C and F), the morphology of the cells and their contact with substrate were similar to those of untreated control cells (Fig. 1, A and C).

A similar study was performed with the mast cell lysate; the results are illustrated in Figure 2. The exposure of osteoblasts to mast cell lysate resulted in a retraction of cells on the substrate (Fig. 2B). The cells exposed to mast cell lysate pretreated with 5 m*M* PMSF (Fig. 2C) showed similar morphology and cell contract with the substrate as the control untreated cells (Fig. 2A). Figure 3 illustrates scanning electron micrographs of osteoblasts grown on collagenase-digested bone fragment. After 5 days, osteoblasts uniformly covered the surface of collagenase-treated rib fragment (Fig. 3A). A higher magnification of these cells showed a polygonal or strap-like shape with broad interconnecting processes and rare microvilli on the cell surface (Fig. 3B). The addition of mast cell lysate for 6 hr induced the changes in cell-matrix interaction, which resulted in cell elongation (Fig. 3C) and the appearance of multiple microvilli on the cell surface (Fig. 3D).

Figure 4 shows SEM of endosteal lining cells of an isolated rat parietal bone. Before the incubation with mast cell lysate (Fig. 4A), the patterns of cell distribution and cell morphology on the matrix were similar to those seen on bone matrix (Fig. 3A). After the incubation with enzyme preparation for 1 hr, there was a significant cell retraction on the surface of bone matrix (Fig. 4B). After 6 hr of incubation with mast cell lysate (Fig. 4C), bone cells assumed a spherical appearance; there were larger visible areas of collagen matrix between the cells and a marked reduction of cell numbers as a result of cell detachment.

Effect on Viability and Proliferation of Osteoblasts. The viability of osteoblasts was assessed by trypan blue exclusion after detachment of cells from matrix. After enzyme-induced detachment, more than 99% of the osteoblasts were viable cells. SEM of the detached cells after treatment with mast cell lysate or chymase showed a cell morphology similar to that of intact osteoblasts (data not shown). In addition, the viability of osteoblasts was analyzed by reculturing the enzyme-treated cells in BJGb medium with 10% FCS; this resulted in a normal osteoblast proliferation and growth pattern (data not shown). Osteoblast proliferation and mitosis were studied with lower concentrations of chymase to avoid cell detachment from the substrate. Quiescent cells showed insignificant differences in metaphase index compared to untreated control cells; osteoblasts incubated with 5% FCS increased the metaphase index 7- to 10-fold (Table I). Similarly, the addition of chymase (0.2 μg/ml) to osteoblasts in culture (70–80% confluence) had no effect on the number of cells after 5 days of incubation ($1.61 \pm 0.3 \times 10^4$ in control group vs. $1.64 \pm 0.15 \times 10^4$ in chymase-treated group; $n = 3$).

Effect on Cell Attachment. The effect of chymase on the attachment of osteoblasts to fibronectin and vitronectin is shown in Figure 5. It can be seen that

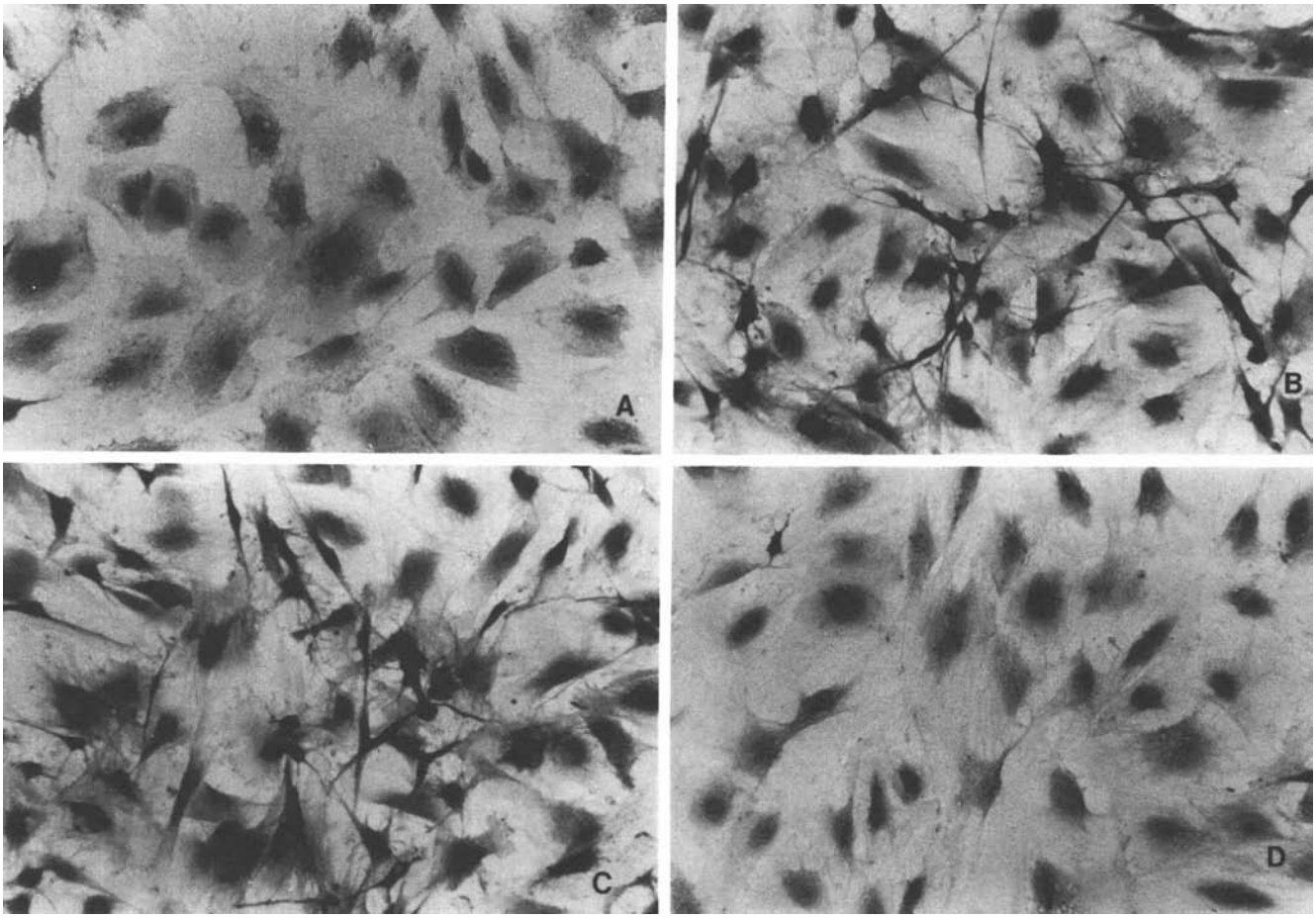

Figure 8. Morphology of rat osteoblasts after exposure to different neutral proteases. Osteoblasts (2×10^4/well) in BGJb medium with 10% FCS were plated onto 24-well dish containing glass coverslips and incubated for 48 hr at 37°C in a 5% CO_2 atmosphere. Before the addition of 0.4 ml of enzyme preparation (1.5 μM; 20 min at 37°C) wells were rinsed with serum-free medium. After incubation, cells were prepared for analysis as described in Materials and Methods. (A) Trypsin; (B) chymotrypsin; (C) chymase; (D) control samples. Magnification ×420. Note the retraction of osteoblasts after treatment with chymotrypsin and chymase and no changes in morphology of cells after exposure to 1.5 μM trypsin.

after a 60-min incubation, half-maximal cell attachment occurred when the culture dishes were coated with approximately 10 μg/ml of fibronectin and 15 μg/ml of vitronectin. These concentrations are equivalent to surface area coating of about 1.56 and 2.3 $\mu g/cm^2$ of fibronectin and vitronectin, respectively. Pretreatment of the matrix proteins with mast cell chymase for 30 min decreased the attachment of osteoblasts. However, after chymase inhibition with antichymotrypsin, the number of attached cells on fibronectin and vitronectin was similar to that in the untreated controls. The time-course experiments over an interval of 1 hr revealed a period of rapid cell attachment up to 20 min; the rate of cell adhesion was slow after that initial period. The chymase-treated wells, coated with either fibronectin or vitronectin, showed a significantly lower degree of cell adhesion for the same time intervals (data not shown). To evaluate the strength of adhesion of mast cell lysate (40 μg/ml) and chymase (2 μg/ml) to plastic or glass and, thus, the possibility of enzyme resilience to BGJb buffer wash, the enzyme preparations were incubated in 24-well plates for 0, 15, 30, and 60 min. The incubation samples were then removed by aspiration and added to osteoblasts in culture. Control samples (zero time) and those exposed to plastic and glass at different time intervals induced similar morphologic changes in cells in culture, as shown in Figures 1B and 2B.

Effect on Cell Spreading. The osteoblast spreading on vitronectin-coated coverslips after exposure to chymase is shown in Figure 6. The osteoblasts seeded on the surface with intact vitronectin (Fig. 6, A and C) had, in most of the cells, a well developed cytoplasm and the central prominence of the nucleus ("fried egg" appearance). Rat osteoblasts seeded on chymase-treated vitronectin (Fig. 6, B and D) were more rounded, had microvili on the cell surface, and displayed a reduction of side-by-side connections. Similarly, the spreading of osteoblasts grown on fibronectin after exposure to chymase was limited, and the cells were poorly attached and spherical (data not shown).

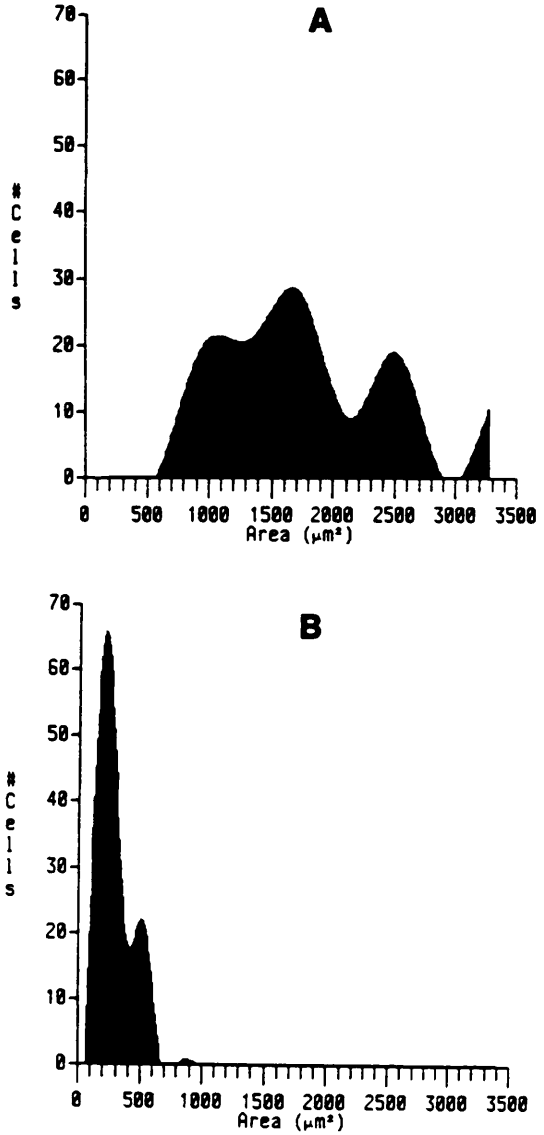

Figure 9. Area of osteoblast cell surface after exposure to mast cell chymase. Osteoblasts (4×10^4/well) in BGJb medium with 0.4% BSA were seeded onto 24-well plates containing coverslips precoated with 0.2 ml of vitronectin (5 μg/ml; 0.5 μg/cm²) for 2 days at 37°C in a 5% CO_2 atmosphere. At the subconfluent stage, cells were exposed to 0.2 ml of chymase (16 μg/ml) for 15 min at 37°C. After incubation, cells were fixed and prepared with actin antibody for immunofluorescent staining (see Materials and Methods). (A) Control cells; (B) chymase-treated cells. Area is expressed in μm². Note a decrease in cell surface after treatment of cell culture with enzyme.

A similar effect of mast cell chymase was seen when bone matrix proteins, obtained from guanidium-EDTA extraction, were used to coat the surface of the coverslips. Mast cell chymase induced alterations in the cell-matrix interaction, which resulted in retraction of cells, a spherical shape, and the appearance of numerous microvili (data not shown).

Figure 7A illustrates the effects of different concentrations of chymase on osteoblast spreading. Trypsin was used in equimolar concentrations for comparison. The increasing concentrations of chymase had a profound effect on cell spreading; at 0.5 μg of enzyme/well, there was a significant inhibitory effect on cell spreading. Additionally, there was a dose-dependency on the number of attached cells; there was a marked decrease in cell attachment ($P < 0.01$) with the increasing concentrations of chymase (Fig. 7B). Figure 8 shows that porcine trypsin (1000 units/mg) had no effect on the interaction between osteoblasts and substrate (Fig. 8A); however, bovine chymotrypsin (1250 units/mg) induced morphologic changes (Fig. 8B) similar to those in osteoblasts treated with chymase (Fig. 8C).

Figure 9 illustrates the results of quantitative analysis of osteoblast surface area after the exposure to chymase. Control cells (Fig. 9A) were larger than enzyme-treated cells (Fig. 9B). This was seen on the graphs as a shift of the enzyme-treated cells to the left, where the total cell surface areas are smaller. The average cell surface area based on digital analysis of actin distribution in the cells was significantly decreased after exposure of the cells to chymase. Digital imaging fluorescence microscopy clearly demonstrated significant differences between the control and enzyme-treated cells. The average area of control osteoblasts was 1864 ± 655 μm², which was significantly higher than 295 ± 129 μm² in enzyme-treated osteoblasts ($P < 0.001$).

Effect on ECM. The deposition of fibronectin in osteoblast cultures occurred in extracellular structures, as visualized by immunofluorescence. Figure 10A shows a fine reticular pattern of fluorescence in the cell culture. Rat osteoblasts in culture treated with mast cell chymase showed a reduction of extracellular fibronectin and the appearance of granular particles, most likely the digested matrix (Fig. 10B). Intracellular staining with antifibronectin antibody remained visible after the exposure of cells to chymase. Both the purified enzyme and the crude enzyme preparations decreased the amount of extracellular fibronectin in osteoblast cultures (data not shown).

Digestion on Matrix Proteins. Figure 11A shows an SDS-PAGE pattern of vitronectin after 60-min incubation with chymase. After 5 min of incubation with the enzyme, intact vitronectin disappeared from the reaction mixture, with a concomitant appearance of polypeptide bands of lower molecular weight. Similarly, fibronectin was digested after 5-min incubation with chymase (Fig. 11B). A longer incubation with chymase resulted in polypeptides of higher mobility; these were apparently the final products of digestion.

Discussion

Degranulation of mast cells in bone has been reported in a variety of conditions (30); most mast cells in bone were found in the periosteum or along the endosteal lining of the trabeculas, in the close vicinity of osteoblasts (31, 32). It is possible that substances released by activated mast cells in bone mediate or

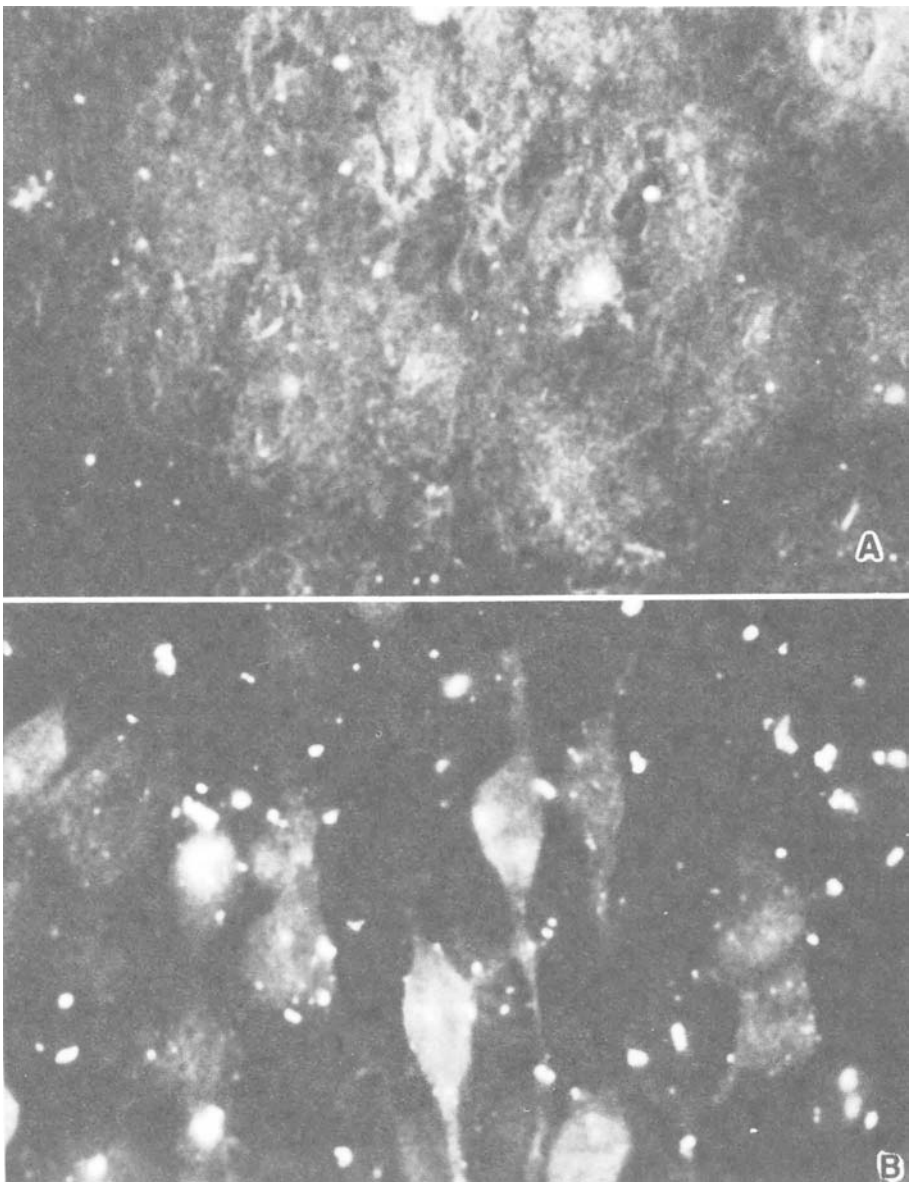

Figure 10. The effect of chymase on matrix fibronectin in osteoblast culture. Osteoblasts (4×10^4 cells/well) in BGJb medium with 10% FCS were seeded in 24-well plates containing coverslips and cultured for 2 to 3 days at 37°C in a 5% CO_2 atmosphere. At the subconfluent stage, cells were rinsed with serum-free medium and incubated with 0.2 ml of either mast cell lysate (150 μg of protein/ml) for 2 h or chymase (33 μg/ml) for 20 min. After incubation, cells were prepared for indirect immunofluorescence as described in Materials and Methods. Control cell culture (A) shows a dense granulo-reticular pattern of fibronectin; after exposure to chymase (B), there was a loss of extracellular fibronectin and an appearance of granular particles, most likely the digested matrix.

modulate the tissue responses to different stimuli. Mast cell chymase, a neutral protease, accounts for approximately half of the protein content of interstitial mast cell granules (8) and is involved in a variety of tissue processes. This enzyme is a mast cell-specific substance with characteristics similar to those of pancreatic chymotrypsin, and it belongs to the family of neutral serine proteases (16, 33). In the respiratory tract, chymase along with trypase, another neutral protease, seems to be involved in the regulation of neuropeptide activity, bronchomuscular tone, and mucus production (34, 35). *In vitro*, chymase converts angiotensin I to angiotensin II (36) and activates bradykinin and kallidin (37). Vartio *et al.* (38) reported an effect of chymase on the degradation of soluble and matrix fibronectin. These authors suggested that chymase may have a function in inflammation by altering the permeability of the basement membrane. Indeed, recent studies by Rubinstein *et al.* (39) indicate that chymase has an amplifying effect on vascular permeability induced by histamine. It has been reported that chymase has a significant proteolytic effect on extracellular matrix proteins; degradation of fibronectin in the matrix was found in the fibroblasts in culture upon exposure to either isolated

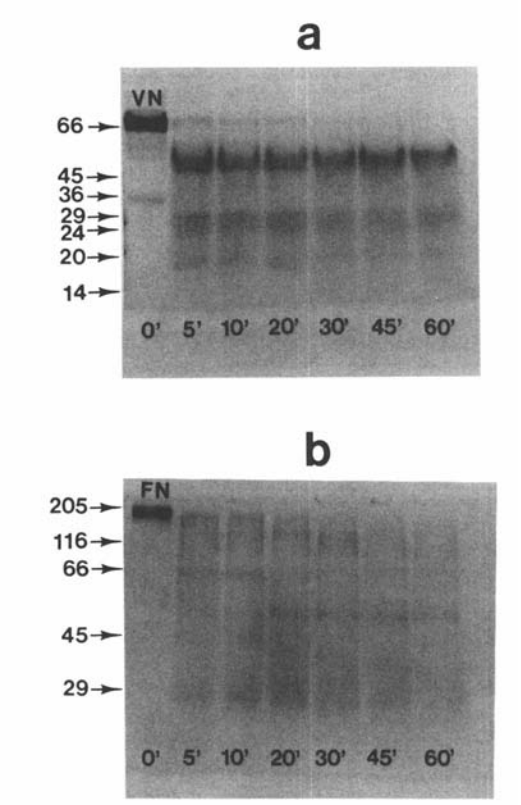

Figure 11. Digestion of matrix proteins by chymase. Vitronectin (33 μg/ml; A) and fibronectin (100 μg/ml; B) were digested by chymase at enzyme/substrate ratios of 1:70 and 1:50, respectively, at 37°C; the digestion products were analyzed by SDS-PAGE. Column 1 shows the starting material; columns 2–7 show the digestion products at given time intervals. Molecular weights are indicated in kilodaltons. FN, fibronectin; VN, vitronectin.

mast cell granules (40) or purified chymase (38). Furthermore, it has been suggested that the effects of chymase may have some importance in the pathogenesis of cartilage erosion (41) and intraosseous invasion of joint tissue in rheumatoid arthritis (42).

The function of mast cells in the bone is less clear, especially in osteoporosis (1, 2) and the healing of fractured bone (6), where numerous mast cells were found in bone specimens. In a previous study we found that mast cell lysate altered the cell-to-substrate interaction of osteoblasts grown on artificial substrata (glass and plastic) (10). In the present study we found similar effects of mast cell lysate on osteoblasts cultured on the biomatrix. When the endosteum of rat parietal bone or osteoblasts grown on collagenase-digested rib fragment were exposed to enzyme preparation, there were changes in the contact between osteoblasts and substrate in the majority of the cells, consisting of cell retraction and the appearance of spherical and spindle-shaped cells. An extended exposure of osteoblasts to mast cell lysate decreased the area of cell contact with the substrate and led to a gradual cell detachment into the culture medium. The effects of a crude enzyme preparation on the osteoblast-matrix interaction were readily reproducible by purified chymase. These observations and the experiments with the neutral protease inhibitors suggested that the neutral protease chymase was the active secretory product of mast cells and could alter the cell-matrix interaction of osteoblasts *in vitro*. Our results support the data of coculture experiments of fibroblasts and vascular endothelial cells with mast cells (43). Greenberg and Burnstock (43) showed a retraction of adjacent cells from the activated mast cells in the short term coculture experiments.

A number of studies have shown that tissue repair in both normal and pathological conditions is linked to an increased activity of neutral proteases. These enzymes are involved in the regulation of proteolysis of ECM and have an important role in tissue remodeling and cell-matrix and cell-cell interactions (44–47). Neutral proteases may release growth factors bound to matrix, such as fibroblast growth factor (48, 49), granulocyte-macrophage colony-stimulating factor (50), interleukin 3 (51), and the bone osteoinductive proteins (52). On the other hand, extracellular matrix alone and in synergism with various systemic and local substances may control the cell function (see review in [53]).

Activated mast cells may have a synergistic function with other cells by the secretion of proteolytic enzymes that are capable of inducing structural changes in the ECM. Proteolytic enzymes of the serine family have been found in a large number of cell types, including neutrophils and lymphocytes (48–50). Serine esterase in cytotoxic T-lymphocytes and cathepsin G in neutrophils contain an amino acid sequence in the catalytic unit that is shared with mast cell chymase (51). Although there is a substantial homology in the amino acid sequence in the catalytic part of the molecule, Western blot analysis and immunoprecipitation studies showed little cross-reactivity with mast cell chymase (51).

Osteoblasts synthesize numerous matrix proteins; some of them are known to be involved in cell adhesion (fibronectin, osteopontin, bone sialoprotein, and thrombospodin) (52). These proteins mediate the attachment and spreading of osteoblasts and other cells on bone matrix. Cell attachment and spreading are vitally important in cell proliferation and differentiation (53). In the present study we found that exposure of osteoblasts to chymase significantly altered the spreading of the cells on vitronectin, fibronectin, and extracted bone matrix proteins. In addition to affecting the cell spreading, chymase had a marked effect on the attachment of osteoblasts. Cellular attachment on vitronectin and fibronectin was significantly reduced by pretreatment of matrix proteins with mast cell chymase. When an equivalent concentration of pancreatic trypsin (0.0001%) was used in the experiments, there was no effect on cell attachment of osteoblasts in culture; higher concentrations of trypsin (0.05–0.25%) used for

routine "trypsinization" altered the interaction between cells and matrix and resulted in cell detachment from the substrate. Additionally, mast cell chymase *in vitro* readily digested soluble fibronectin and vitronectin and had a proteolytic effect on matrix fibronectin in osteoblast cultures. Although the precise role of matrix proteins in the control of cell function in bone is not known, it is likely that neutral proteases, released locally by different cells, may have an effect on the structure of matrix molecules and their interaction with bone cells.

In conclusion, our findings indicate that mast cell chymase has an effect on matrix proteins and alters osteoblast-matrix interaction *in vitro*. This suggests that mast cells, through the protease activity, may have a role in bone remodeling.

This work was supported in part by Lynn Wolfson and the Loulyfran Wolfson Foundation.

We thank Drs. Gay Howard and Hilda Lo for valuable discussions, Dr. Margita Zakarija for determination of cAMP, Sue Decker and Steve H. Hart for technical assistance, and Thelma Eddie for typing the manuscript.

1. Fallon MC, Whyte MP, Graig B, Teitelbaum SL. Mast cell proliferation in postmenopausal osteoporosis. Calcif Tissue Int **35**:29–31, 1983.
2. Frame B, Nixon RK. Bone-marrow mast cells in osteoporosis of aging. N Engl J Med **279**:626–630, 1968.
3. Neiman RS, Bischel MD, Lukes RJ. Uremia and mast cell proliferation. Lancet **1**:959–962, 1972.
4. Peart KM, Ellis HA. Quantitative observations on iliac bone marrow mast cells in chronic renal failure. J Clin Pathol **28**:947–955, 1975.
5. Urist MR, McLean FC. Accumulation of mast cells in endosteum of bones of calcium-deficient rats. AMA Arch Pathol **63**:234–251, 1957.
6. Lindholm R, Lindholm S, Liukko P, Paasimaki J, Isokaanta S, Rossi R, Autio E, Tamminen E. The mast cell as a component of callus in healing fractures. J Bone Joint Surg **51B**:148–155,1969.
7. Severson AR. Mast cells in areas of experimental bone resorption and remodeling. Br J Exp Pathol **50**:17–21, 1969.
8. Schwartz LB, Austen KF. Structure and function of the chemical mediators of mast cells. Prog Allergy **34**:271–321, 1984.
9. Gordon JR, Burd PR, Galli SJ. Mast cells as a source of multifunctional cytokines. Immunol Today **11**:458–464, 1990.
10. Banovac K. Mast cell induced morphological changes of bone cells in culture. In: Christiansen C, Overgard K, Eds. Osteoporosis 1990. Copenhagen: Osteopress, Vol **1**: pp274–276, 1990.
11. Banovac K, Neylan D, Leone J, Ghandur-Mnaymneh L, Rabinovitch A. Are the mast cells antigen presenting cells? Immunol Invest **18**:901–906, 1989.
12. Young JE, Liu CC, Butler G, Cohn ZA, Galli SJ. Identification, purification and characterization of a mast cell-associated cytolytic factor related to tumor necrosis factor. Proc Natl Acad Sci USA **84**:9175–9179, 1987.
13. Schick B, Austen KF, Schwartz LB. Activation of rat serosal mast cells by chymase, an endogenous secretory granule protease. J Immunol **132**:2571–1577, 1984.
14. Schwartz LB, Reidel C, Schratz JJ, Austen KF. Localization of carboxypeptidase A to the macromolecular heparin proteoglycan-protein complex in secretory granules of rat serosal mast cells. J Immunol **128**:1128–1133, 1982.
15. Weber K, Osborn M. The reliability of molecular weight determinations by dodecyl-polyacrylamide gel electrophoresis. J Biol Chem **244**:4406–4412, 1969.
16. Schechter NM. Human chymase. In: Schwartz LB, Ed. Neutral Proteases of Mast Cells. Monographs on Allergy. Basel: Karger, Vol **27**: pp114–131, 1990.
17. Yatogho T, Izumi M, Kashiwagi H, Hayashi M. Novel purification of vitronectin from human plasma by heparin affinity chromatography. Cell Struct Funct **13**:281–292, 1988.
18. Termine JD, Belcourt AB, Christner PJ, Conn KM, Nylen MU. Properties of dissociatively extracted fetal tooth matrix proteins. J Biol Chem **255**:9760–9768, 1980.
19. Termine JD, Keinman HK, Whitson SW, Conn KM, McGravey M, Martin GR. Osteonectin, a bone-specific protein linking mineral to collagen. Cell **26**:99–105, 1981.
20. Termine JD, Belcourt AB, Conn KM, Kleinman HK. Mineral and collagen-binding proteins of fetal calf bone. J Biol Chem **256**:10403–10408, 1981.
21. Wong GL, Cohn DV. Target cells in bone for parathormone and calcitonin are different. Enrichment for each cell type by sequential digestion of mouse calvaria and selective adhesion to polymeric surfaces. Proc Natl Acad Sci USA **72**:3167–3171, 1975.
22. Majeska RJ, Rodan SB, Rodan GA. Parathyroid hormone-responsive clonal cell lines from rat osteosarcoma. Endocrinology **107**:1484–1503, 1980.
23. Bourdin NA, Ruoslahti E. Tenescin mediates cell attachment through an RGD-dependent receptor. J Cell Biol **108**:1149–1155, 1989.
24. Oliver MH, Harrison NK, Bishop JE, Cole PJ, Laurent GJ. A rapid and convenient assay for counting cells cultured in microwell plates: Application for assessment of growth factors. J Cell Sci **92**:513–518, 1989.
25. Grinnell F, Hay DG, Mitter D. Cell adhesion and spreading factor. Partial purification and properties. Exp Cell Res **110**:175–190, 1977.
26. Brinkley BR, Fistel SH, Marcam JM, Pardue RL. Microtubules in cultured cells: Indirect immunofluorescent staining with tubulin antibody. Int Rev Cytol **63**:59–80, 1980.
27. Koren E, Frazen J, Fugate RD, Alaupovic P. Analysis of cholesterol ester accumulation in macrophages by the use of digital fluorescence microscopy. Atherosclerosis **38**:178–184, 1990.
28. Banovac K, Ghandur-Mnaymneh L, Leone J, Neylan D, Rabinovitch A. Intrathyroidal mast cells express major histocompatibility complex class-II antigens. Int Arch Allergy Immunol **90**:43–46, 1989.
29. Malinin GI. Sodium bisulfite addition reaction and toluidine blue staining of deoxyribonucleic acid after Feulgen hydrolysis. J Histochem Cytochem **23**:974–977, 1975.
30. McKenna MJ, Frame B. The mast cell and bone. Clin Orthop **200**:226–231, 1985.
31. Selye H. The mast cells. Washington, DC: Butherworths, 1965.
32. Endo Y, Kikuchi T, Nakamura M, Shinoda H. Determination of histamine and polyamines in calcified tissues of mice: Contribution of mast cells and histidine decarboxylase to the amount of histamine in the bone. Calcif Tissue Int **51**:67–71, 1992.
33. Caughey GH. Tryptase and chymase in dog mast cells. In: Schwartz LB, Ed. Neutral Proteases of Mast Cells. Monographs on Allergy. Basel: Karger, Vol **27**: pp67–89, 1990.
34. Gold WM, Lazarus SC. Mast cells and cell-to-cell interactions in airways. Am Rev Respir Dis **143**:S61–S63, 1991.
35. Caughey GH. Roles of mast cell trypase and chymase in airway function. Am J Physiol **257**:L39–L42, 1989.
36. Reilly GF, Tewksburry DA, Schechter NB, Travis J. Rapid

conversion of angiotensin I to angiotensin II by neutrophil and mast cell proteinases. J Biol Chem **257**:8619–8623, 1982.
37. Reilly GF, Schechter NB, Travis J. Inactivation of bradykinin and kallidin by cathepsin G and mast cell chymase. Biochem Biophys Res Commun **127**:443–456, 1985.
38. Vartio T, Seppa H , Vaheri A. Susceptibility of soluble and matrix fibronectins to degradation by tissue proteases, mast cell chymase and cathepsin G. J Biol Chem **256**:471–477, 1981.
39. Rubinstein I, Nadel JA, Graf PD, Caughey GH. Mast cell chymase potentiates histamine-induced weal formation in the skin of rag weed-allergic dogs. J Clin Invest **86**:555–559, 1990.
40. Atkins FM, Friedman MM, Subba Rao PV, Metcalfe DD. Interactions between mast cells, fibroblasts and connective tissue components. Int Archs Allergy Appl Immunol **77**:96–102, 1985.
41. Bromley M, Fisher WD, Woolley DE. Mast cells at sites of cartilage erosion in the rheumatoid joint. Ann Rheum Dis **43**:76–79, 1984.
42. Crisp AJ, Chapman CM, Kirkham SE, Schiller AL, Krane SM. Articular mastocytosis in rheumatoid arthritis. Arthritis Rheum **27**:845–851, 1984.
43. Greenberg G, Burnstock B. A novel cell-to-cell interaction between mast cells and other cell types. Exp Cell Res **147**:1–13, 1983.
44. Mullins DE, Rohrlich ST. The role of proteinases in cellular invasiveness. Biochim Biophys Acta **695**:177–187, 1983.
45. Bond JS, Butler PE. Intracellular proteases. Annu Rev Biochem **56**:333–364, 1987.
46. Saksela O, Rifkin DB. Cell-associated plasminogen activation: Regulation and physiological functions. Annu Rev Cell Biol **4**:93–126, 1988.
47. Moscatelli D, Rifkin DB. Membrane and matrix localization of proteinases: A common theme in tumor cell invasion and angiogenesis. Biochim Biophys Acta **948**:67–85, 1988.
48. Vlodavsky I, Folkman J, Sullivan R, Fridman R, Ishai-Michaeli R, Sasse J, Klagsbrun M. Endothelial cell-derived basic fibroblast growth factor: Synthesis and deposition into subendothelial extracellular matrix. Proc Natl Acad Sci USA **84**:2292–2296, 1987.
49. Baird MY, Lang N. Fibroblast growth factors are present in the extracellular matrix produced by endothelial cells *in vitro*: Implication for a role of heparinase like enzymes in the neovascular response. Biochem Biophys Res Commun **142**:428–435, 1987.
50. Gordon MY, Riley GP, Watt SM, Greaves MF. Compartmelization of a haematopoietic growth factor (GM-CSF) by glycosaminoglycans in the bone marrow microenvironment. Nature **326**:403–405, 1987.
51. Klagsbrun M. The affinity of fibroblast growth factors (FGFs) for heparin. Current Opin Cell Biol **2**:857–863, 1990.
52. Sampath TK, Coughlin JE, Whetstone RM, Banach D, Corbett C, Ridge RJ, Ozkaynak E, Opperman H, Rueger DC. Bovine osteogenic protein is composed of dimers of OP-1 and BMP 2A, two members of the transforming growth factor-beta superfamily. J Biol Chem **265**:13198–13205, 1990.
53. Getzen RH, Pienta KJ, Coffey DS. The tissue matrix: Cell dynamic and hormone action. Endocr Rev **11**:399–415, 1990.
54. Masson D, Tschopp JA. family of serine esterases in lytic granules of cytotoxic T-lymphocytes. Cell **32**:679–685, 1987.
55. Pasternack MS, Eisen HN. A novel serine esterase expressed by cytotoxic T-lymphocytes. Nature **314**:743–751, 1985.
56. Kramer MD, Binninger L, Schirrmacher V, Moll H, Prester M, Nerz G, Simon MM. Characterizstion and isolation of a trypsin-like serine protease from a long term culture cytotoxic cell line and its expression by functionally distinct T cells. Immunology **136**:4644–4651, 1986.
57. Salverson G, Farley D, Shuman J. Molecular cloning of human cathepsin G: Structural similarity of mast cell and cytotoxic T lymphocyte proteases. Biochemistry **26**:2289–2293, 1987.
58. Heinegard D, Oldberg A. Structure and biology of cartilage and bone matrix noncollagenous macromolecules. FASEB J **3**:2042–2052, 1989.
59. Rouslahti E, Pierschbacher MD. New perspectives in cell adhesion: RGD and integrins. Science **238**:491–497, 1987.